

A Simple, Yet Realistic Model for the Formation of Arctic Stratus Clouds—A Case Study

O. Lie-Svendsen
Norwegian Defense Research Establishment
Kjeller, Norway

Q. Zhang, J. Simmons, and K. Stamnes
Geophysical Institute
University of Alaska, Fairbanks

Introduction

We have developed a one-dimensional radiative-convective model with detailed cloud microphysics, and used it to study the formation of Arctic Stratus clouds (ASC). The model contains detailed radiative and microphysical modules, and it provides a self-consistent treatment of the interaction between radiative and cloud microphysical processes

important for cloud formation. The radiative transfer code is coupled to the microphysics module that has been developed to simulate the detailed cloud droplet activation and evaporation processes, using the full droplet size distribution. In addition, the model includes convective adjustment, which implies mixing of droplet spectra.

In this case study, we initialize the model using the temperature and humidity profiles shown in Figure 1, which

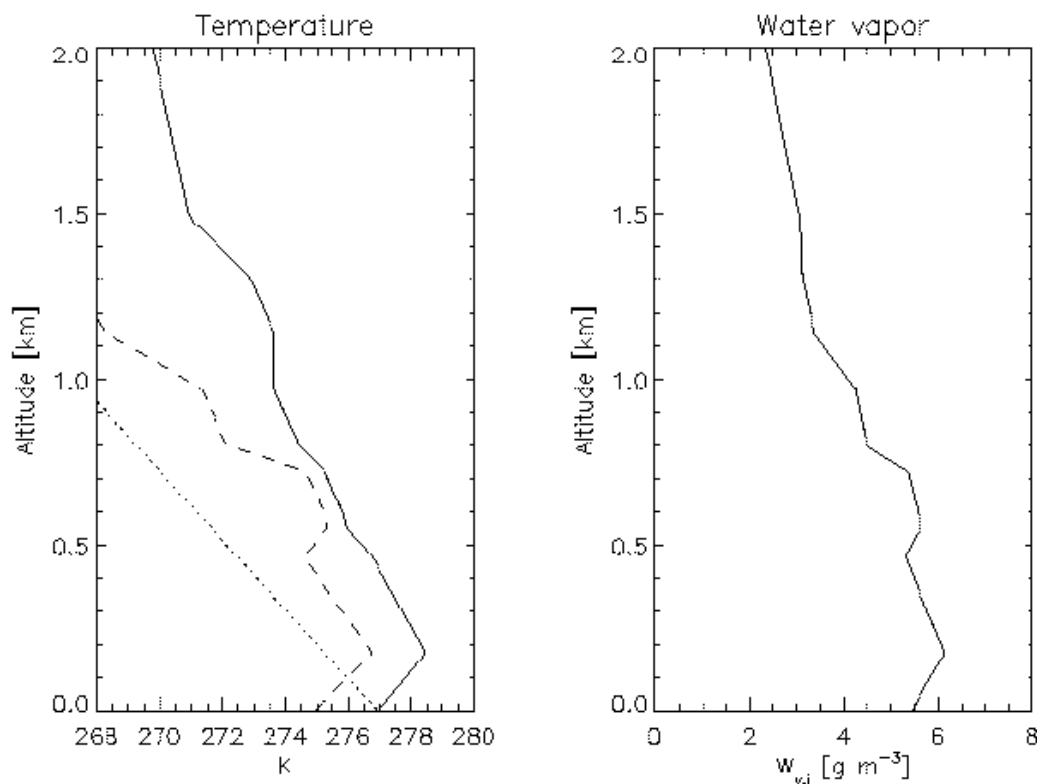


Figure 1. Balloon sounding from Barrow at 00 GMT, June 10, 1980, which is used to initialize the model. The solid line in the left panel is the actual temperature, the dashed line is the dew point temperature, T_c ; and the dotted line is the lapse rate for dry air.

have been obtained from a balloon sounding from Barrow, Alaska. We use 200 altitude grid points, with 10-m resolution below 1 km (where the cloud forms) and coarser above. We adopt an initial cloud condensation nuclei (CCN) spectrum measured in April 1992, during the LEADDEX experiment (Hegg et al. 1995). This spectrum can be approximately represented by a power law (Twomey 1977)

$$N_{\text{CCN}} \approx c(100s)^\kappa$$

where s is the supersaturation, $\kappa=0.34$, and $c=1.28 \times 10^8 \text{ m}^{-3}$. The model follows the evolution of this column (which is clear air initially) for 16.5 hours. A cloud forms 6.5 hours into the calculation at 700 m altitude (where the initial temperature and dew point temperature are less than 1 K apart).

Figure 2 shows how the temperature and three moments of the droplet distribution (ratio of liquid water to water vapor, droplet density, and equivalent radius) evolve with time after the cloud has formed. Initially the air cools slowly, and even 6 hours into the simulation (just prior to cloud formation) the temperature has decreased by less than 1 K. The shape of the temperature profile remains almost unchanged compared to the initial profile, implying that the cooling rate is nearly independent of altitude. Once the cloud forms, the cooling rate increases drastically in the cloud region and a temperature inversion quickly develops, and deepens, due to cloud-top infrared cooling. Ten hours after cloud formation we find that the cloud top remains at its initial 700 m location, capped by a steep inversion, but the cloud base has extended to about 250 m.

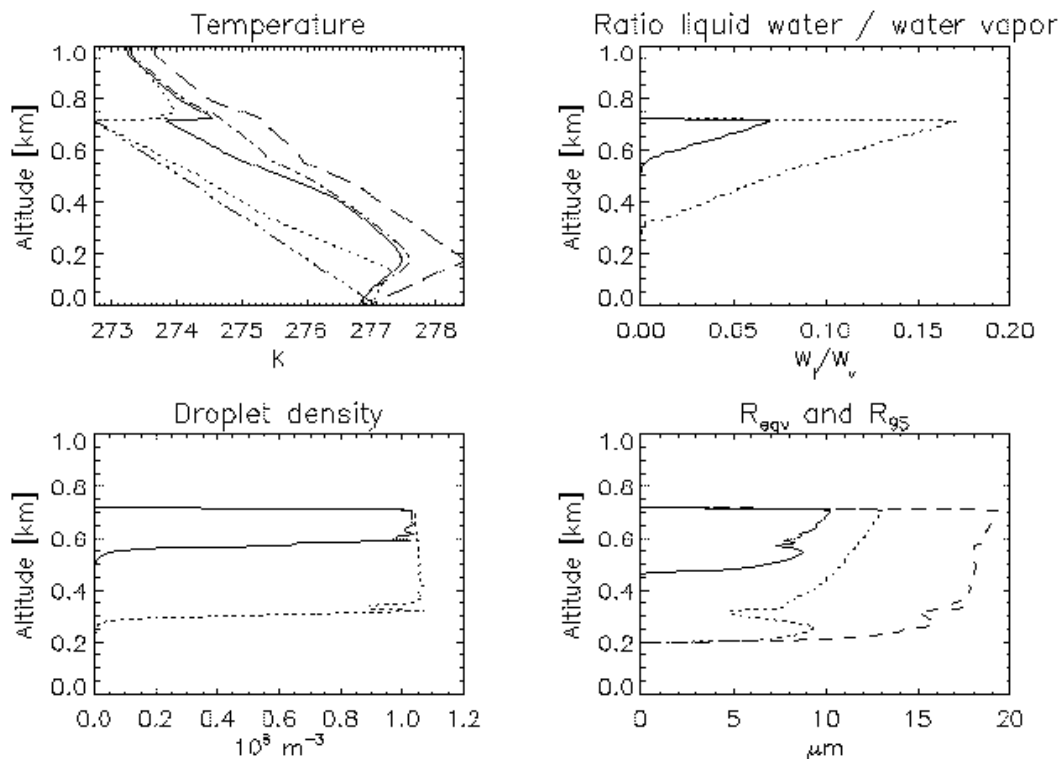


Figure 2. Temperature, ratio of liquid water to water vapor, droplet density, and equivalent radius at $t=28$ minutes before cloud formation (dash-dot line), $t=1.6$ (solid line), and 10 hours (dotted line) after cloud formation. The dash-dot-dot-dot line shows the corresponding lapse rate temperature after 10 hours, extrapolated downwards from the actual temperature at 770 m altitude. The initial temperature from the sounding is also shown (long dashes). In the lower right panel, the dashed line denotes r_{95} after 10 hours, where r_{95} is the radius below which 95% of the liquid water is contained.

Within the modeled cloud the liquid water content (LWC) generally increases with altitude, as one expects from adiabatically rising air. The equivalent radius also shows a general increase with altitude, although the trend is not as pronounced. By contrast, the droplet density shows no such trend, being roughly independent of altitude. This implies that the increase in LWC is related to an increase in droplet size rather than droplet density. The maximum supersaturation reached anywhere during the model run was 0.71 %.

Figure 3 shows the droplet size distribution at the end of the run, between the cloud top at 710 m and the cloud base

250 m. The distribution has been collected in 15 equidistant bins with mean diameter separated by $3.13 \mu\text{m}$, corresponding to the resolution of the Forward Scattering Spectrometer Probe used in the ASC experiment (Tsay and Jayaweera 1984). At the end the model has produced fairly broad size distributions in the upper parts of the cloud. The broad size distributions can be attributed to the mixing taking place throughout the cloud. Near the bottom of the cloud, the distribution is generally clustered around a single peak at about $10 \mu\text{m}$ diameter or less. In the upper parts of the cloud, the much broader distribution typically shows several peaks between 10 and $30 \mu\text{m}$, and a tail extending to about $40 \mu\text{m}$.

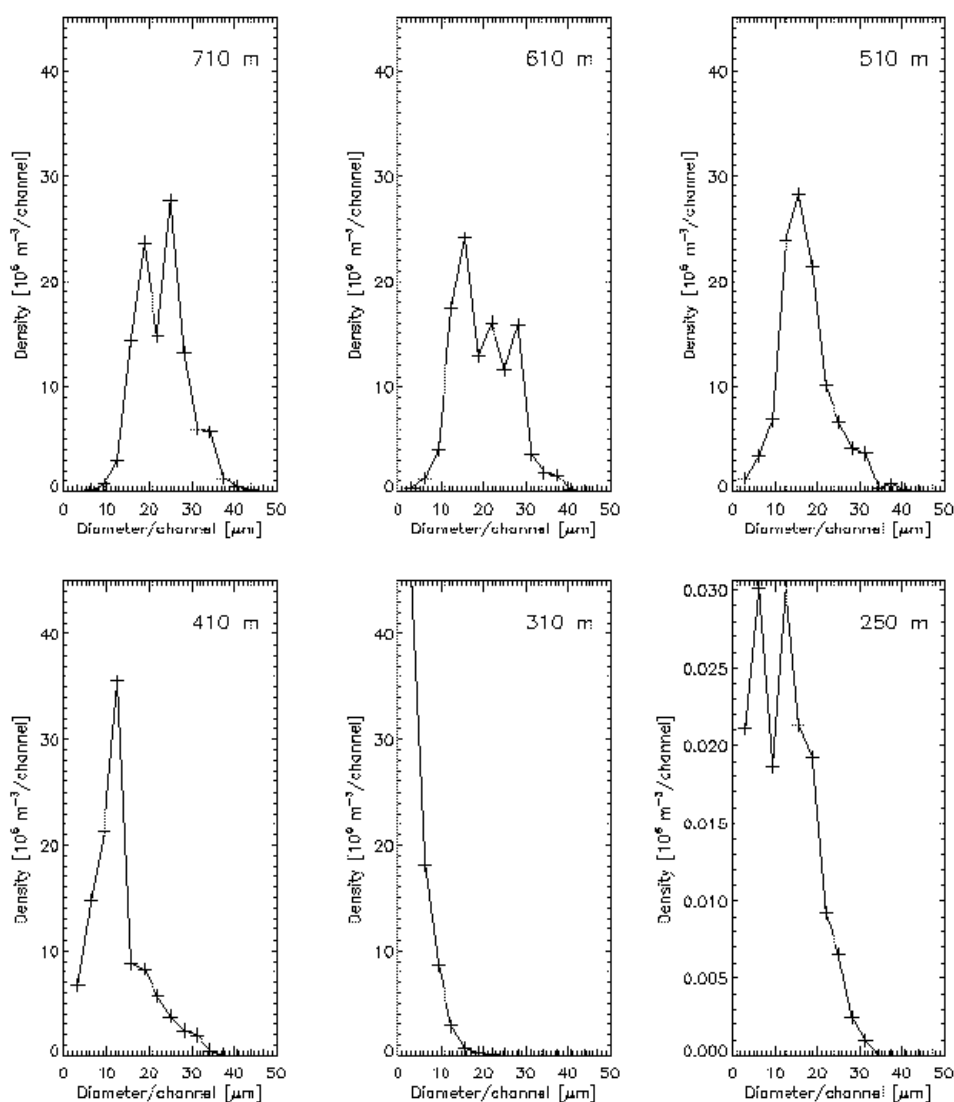


Figure 3. The droplet size distribution 10 hours after cloud formation. The distribution has been collected in 15 equidistant bins with mean diameter $3.13 \mu\text{m}$ apart, with the pluses indicating the center of each bin.

Figure 4 shows the warming/cooling rates due to solar and infrared radiation. The very strong infrared cooling near the cloud top is responsible for the deep inversion developing here. The lower panels demonstrate that even with 10-m resolution the model is not able to fully resolve the radiation field at the cloud top, with an almost discontinuous jump both in solar and infrared heating rates.

Summary of Results

- Cloud top infrared (IR) cooling causes a strong temperature inversion to develop.
- The cloud top cooling maintains vigorous mixing throughout the cloud at all times during the simulation; as a result, the droplet density is nearly independent of altitude.

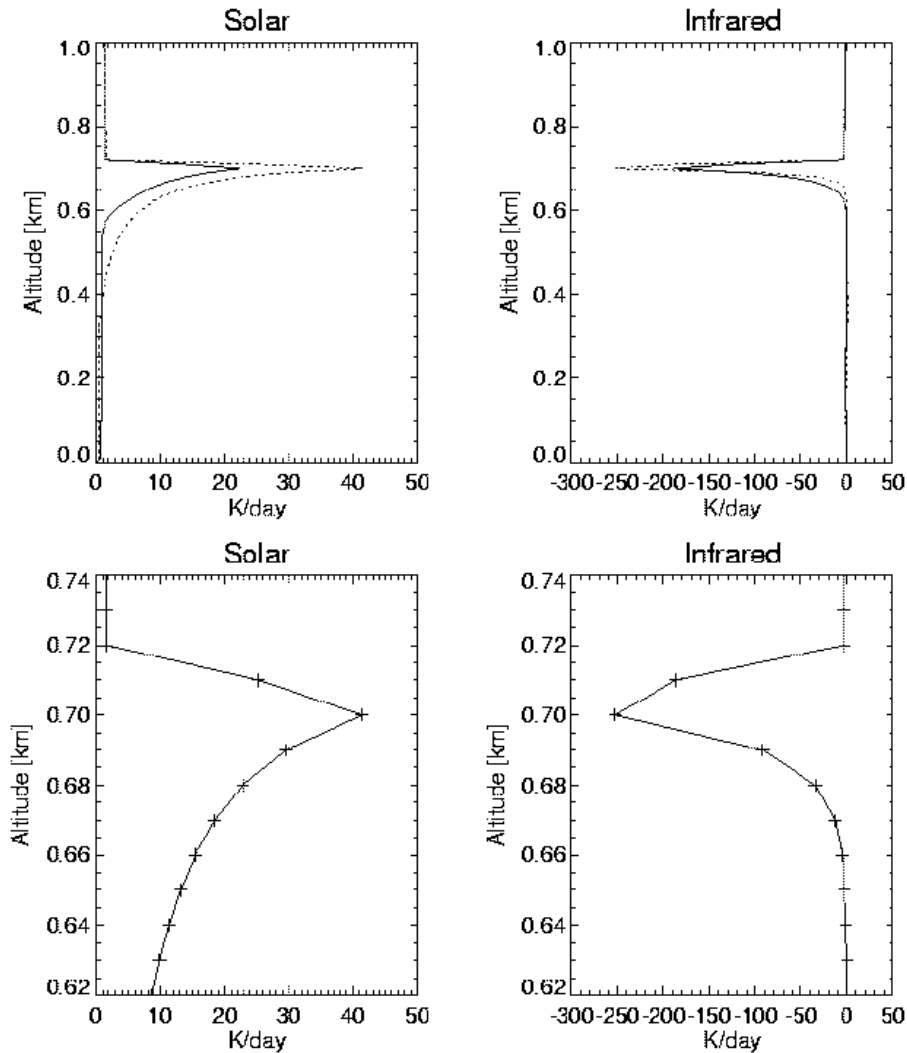


Figure 4. Warming/cooling rates from solar and infrared radiation. The solid lines are 1.6 hours after first cloud formation and the dotted lines at the end of the simulation. The lower panels show the same warming/ cooling rates near the cloud top at the end of the run, with the pluses indicating the actual grid points used in the computation. The change in temperature due to latent heat release/absorption is not included in this figure.

- The LWC increases with altitude, close to the adiabatic value.
- Since the droplet density is nearly independent of altitude, the increase in liquid water is related to an increase in droplet size rather than droplet density.
- The droplet size distribution typically shows a single mode distribution in the lower parts of the cloud, and broadens with altitude, often with several peaks in the upper parts of the cloud. The size distribution also tends to broaden with time.
- The CCN spectrum determines the number of cloud droplets (the Twomey effect), but is less important for the shape of the droplet size distribution, which is largely determined by the mixing of cloud layers.

These results are both qualitatively and quantitatively in good agreement with in situ observations of ASCs. The main deficiency of the model is that it tends to produce droplets that are too large compared to observations (up to 50 μm near cloud top). This is probably caused by the lack of cloud dissipation mechanisms in the model (coalescence, gravitational settling).

The results suggest that a very simple model including only radiation, cloud microphysics and parameterized vertical mixing is able to reproduce the general features of ASCs. They also underscore the important role that radiation plays in the Arctic, and indicate that the treatment of these clouds in climate models may be simplified.

References

- Hegg, D. A., R. J. Ferek, and P. V. Hobbs, 1995: Cloud condensation nuclei over the Arctic ocean in early spring. *J. Appl. Meteor.*, **34**, 2076-2082.
- Twomey, S., 1977: *Atmospheric Aerosols*. Elsevier Scientific Publishing.
- Tsay, Si-Chee, and K. Jayaweera, 1984: Physical characteristics of Arctic stratus clouds. *J. Climate Appl. Meteor.*, **23**, 584-596.